FUPRE Journal of Scientific and Industrial Research
Vol.6, (1), 2022
ISSN: 2579-1184 (Print) ISSN: 2578-1129 (Online)

Design and Development of Switched Reluctance Motor Towards Minimizing Torque Ripples and Acoustic Noise

B. O. Akinloye[1] and B. E. Nyong-Bassey[1]
[1]Department of Electrical and Electronics Engineering, Federal University of Petroleum Resources, Effurun
[1]akinloye.benjamin@fupre.edu.ng and [1]nyongbassey.bassey@fupre.edu.ng

Abstract

Recently, the use of switched reluctance motors (SRMs) has considerably increased due to technological developments of systems and devices requiring more control. More so, peculiar features of SRMs such as robustness, reliability, low cost construction makes it ideal for applications in ventilation systems, pumps and systems that require high speed. However, SRMs have the problem of torque ripples and high acoustic noise from design and development stage. The torque ripples experienced by the SRM ensues as the rotor tries to align itself to an excited phase on the stator. Therefore, the aim of this paper is to design and develop a 3 phase, 6/4 switched reluctance motor in order to reduce the issues of torque ripple and acoustic noise. Finite element analysis software (Ansys-Maxwell) was used to carry out the nonlinear electromagnetic transient analysis of the motor while the control topology used was simulated using the MATLAB software. The design stages involved suitable assumptions which were made for the stator design, winding design and rotor design. The results from the analysis and performance of the motor have been presented in the work. The magnetic field plot of the developed motor does not present saturation effect on any part.

Keywords: Switched Reluctance Motor, Torque, Rotor, Stator

1. Introduction

More recently, the demand for a variable speed drive by consumers with germane concerns bothering on efficiency and cost has been on the increase (Krishnan, et al, 2005 and Kim et al, 2012).On the one hand, single-phase and three-phase motors which have controllable switched based inverters have been proposed for variable speed drive operations. Nevertheless, the cost of manufacturing such drive systems has made it less desirable (Krishnan, 2001).On the other hand, switched reluctance motors (SRMs) are known to be of simple construction and low cost (Kim et al, 2012). SRMs neither have neither brushes nor commutators with the absence of windings or magnets on its rotor, while the windings on its stator are only concentrated. Thus, these conditions are advantageous and made it to be the lowest cost machine (Kim et al, 2012). However, torque performance of the switched reluctance motor exhibit pulsations due to the electronics switching of the phases of the motor during excitation.

Several authors have proposed varied strategies to enhance the torque

performance of SRMs. In Sanches and Santisteban, (2015) the performance evaluation of a 6/4 switched reluctance motor considering the contribution of the mutual inductances on the production of torque was presented. The dependence of electromagnetic torque of switched reluctance motor (SRM) was shown in (Sheth and Rajagopal, 2005) by calculating the flux linkage characteristic of SRM using flux tube method. A novel electromagnetic actuator with 2 degrees of freedom for rotational and linear actuation was presented in (Sato, 2007, Zou et al, 2014 and Cao et al 2020). The electromagnetic actuators are based on switched reluctance motor which has its torque and thrust controlled independently. Steady state and dynamic analysis of toroidal winding switched reluctance motor driven by 6-switch converter is presented (Ji-Young et al, 2006). It was claimed that the cost of production of the 6-switch converter is cheaper than the asymmetric control of switched reluctance motor. Time-stepped voltage source finite element method was used in analysing switched reluctance motor with a consideration to the free-wheeling diode and dc-link voltage ripples (Choi et al, 2005 and Bao et al 2016). Trade-off between conventional design method of SRM which prioritize saliency ratio (Allirani et al 2018) and a new method used which prioritizes reduction of saliency ratio and eventually back EMF was presented (Fan and Lee 2020). The impact of electrical steel punchings on the performance of SRM was carried out by (Chiang et al, 2015). Farmahini et al 2020 enhanced SRM torque by the addition of permanent magnet. The design of switched reluctance motor goes beyond the output equation that is used for designing general motors. The purpose of this paper is to design and develop a 6/4 switched reluctance motor. It has six (6) poles on the stator and four (4) on the rotor to produce reluctance torque. Switched reluctance motor (SRM) is different from other conventional ac motors in the sense that it has different number of poles on the stator and the rotor. SRM is simply a type of stepper motor that runs by reluctance torque. The excitation is applied only to the windings on the stator and not to the moving part. This requires switching system in order to deliver the power to different windings on the stator.

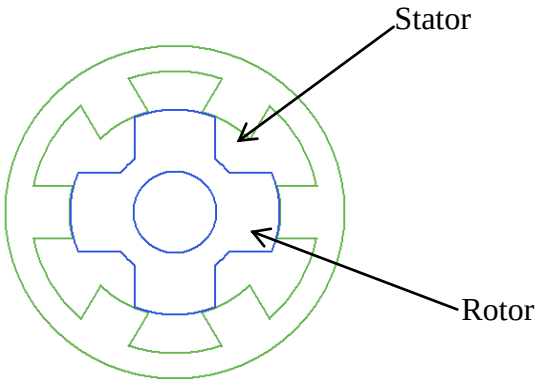

Figure 1. Schematic diagram of 6/4 Switched Reluctance Motor

The stator and rotor are made up of silicon steel stampings. The poles are projected inward and carry the field coils. In order to make the magneto motive force (MMF) to be additive, the windings on the stator are connected such that the opposite coils are connected in series and these group of coils form the phase windings. The motor terminals are connected to the output terminals of power switching circuit. The poles are projecting outward. There is always provision for a rotor position sensor in order to know the appropriate time of firing the stator winding and hence influence the turning on and off of the switching circuit. Figure 2 describe the basic blocks of operation of SRM

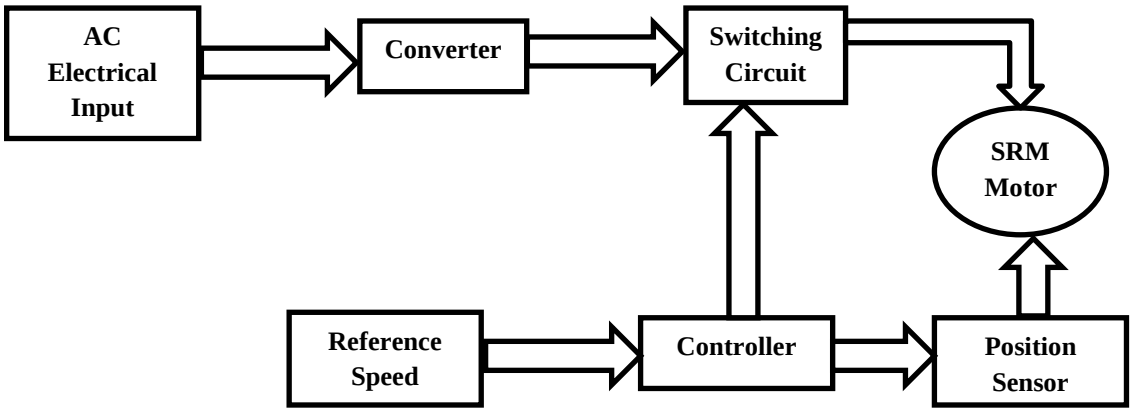

Figure 2. Block Diagram of SRM

2. Design of Switched Reluctance Motor

The design of SRM forms a major source of acoustic noise due to radial forces which causes deformation in the stator. Hence, making the design to be rigid helps to reduce this deformation. As earlier stated, the air gap of SRM is non-uniform. The know parameters of the motor to be designed are presented in Table 1.

Table 1: SRM design parameters.

Terminal voltage (V_s)	220V
Frequency	50 Hz
Rated output power ($\mathbf{P_0}$)	746 W
Number of phases (m)	3
Number of stator poles (N_s)	6
Number of rotor poles (N_r)	4
Rated output Speed of the motor (n_s)	1500 rpm or 25 r.p.s

The following assumptions are made for the design of the motor; Stator flux density (B_s) = 1.7T, efficiency (k_e) =0.8, duty cycle (K_d) = 1, specific electric loading

(A_s) = 25,000AT/m, packing factor = 0.9, current density (J_c) = 4A/mm

The output equation for the SRM is given as;

$$P_0 = K_d \times K_e \times K_1 \times K_2 \times B_S \times A_S \times L \times D^2_i \times N_{rt} \quad (1)$$

Length of the stator core (L) is expressed as;

$$L = 0.45 D_i \quad (2)$$

$$K_1 = \frac{\pi^2}{120} = 0.082 \quad (3)$$

The value of K_2 varies from 0.65 to 0.75($0.65 \leq K_2 \geq 0.75$); so, for this work, $K_2 = 0.7$ is taken.Therefore, substituting equations (2) and (3) in equation (1) and using the parameters in Table 1, internal diameter D_i is obtained as

$$D_i = 0.0827m = 82.7mm$$

$$L = 0.45 \times 0.0827 = 0.0372\text{m} = 37.2\text{mm}$$

Rated output torque equation for the SRM is calculated using equation (4)

$$T = K_d \times K_e \times K_2 \times B_S \times A_S \times L \times D^2_i \times \frac{\pi}{4} \quad (4)$$

$$T = 4.76N.m$$

2.1 Pole Pitch and Arc

The width of the pole arc provides an agreement between the regularity of the torque and induction ratio which correlates to the torque density of the machine. Smaller poles create more room for windings which increases the machine efficiency and they also provide a higher inductance ratio but at the same time, increase the torque ripple. Larger pole arcs on the other hand improve the torque pulsations, although at the cost of the machine efficiency. So, the idea is a trade of between the efficiency and torque pulsation minimization. Furthermore, when the rotor pole arc is greater than that of the stator, negative torque production is avoided and hence, reduction in the torque.

i. tator pole pitch(τ_{sp})

$$\tau_{sp} = \frac{360}{6} = 60^0$$

ii. Rotor pole pitch(τ_{rp})

$$\tau_{rp} = \frac{360}{4} = 90^0$$

iii. Stator pole arc (β_s)

$$\beta_s = \frac{\pi \times 4}{N_s \times N_r} = \frac{180 \times 2}{4 \times 6} = 30^0$$

iv. Rotor pole arc(β_r)

As stated earlier, the rotor pole arc must be greater or at least equal to the stator pole arc. For this motor, a variation of 6% between the rotor pole arc and the stator pole arc is assumed. Thus

$$\beta_r = 30 \times \frac{6}{100} = 1.8$$

$$\beta_r = 30 + 1.8 = 31.8^0$$

2.2 Design Variables

The design variables are the electromagnetic value for the geometry of the motor that have to be evaluated. These include Width of the stator pole (w_{sp}), Width of rotor pole (w_{rp}), Stator yoke height (h_{sy}), Rotor yoke height (h_{ry}), Height of the stator pole (h_{sp}), Length of air gap (g), Height of the rotor pole (h_{rp}).

a) Stator pole width (w_{sp})

The stator pole width is expressed in terms of the bore diameter and stator pole arc.

$$\text{Wsp} = D_i \times \sin\frac{\beta_s}{2} \quad = 21.40mm$$

b) Rotor pole width (w_{rp})

The rotor pole width is expressed in terms of the bore diameter and the rotor pole arc.

$$\text{Wrp} = D_i \times \sin\frac{\beta_r}{2} = 22.65mm$$

c) Stator yoke height (h_{sy})

The stator yoke height, also known as the stator back iron thickness is approximately equal to half of the stator pole width because the magnetic flux flowing through the back iron splits into half. The stator yoke height has a range which is stated as;

$W_{sp} > h_{sy} \geq 0.5 \times W_{sp}$; thus,

$$h_{sy} = 0.6 \times w_{sp}$$

$$h_{sy} = 0.6 \times 21.40 = 12.84mm$$

d) Rotor yoke height (h_{sy})

The rotor yoke height, also known as the rotor back iron thickness is assumed to have the same value as that of the stator yoke height since it has the same flux flowing through the rotor pole. It has a range of;

$0.5W_{sp} < h_{sy} < 0.75W_{rp}$, thus,

$$h_{sy} = 0.6 \times w_{sp} = 12.84mm$$

e) Stator pole height (h_{sp})

The stator pole height is calculated by subtracting the bore diameter and twice the stator yoke height from the outer diameter. Mathematically expressed as;

$$D_0 = D_i + 2h_{sy} + 2h_{sp}$$

Where,

$$D_0 = \frac{D_i}{k} \quad and \quad (0.4 \leq k \geq 0.7)$$

$$D_0 = \frac{82.7}{0.5} = 165.4mm$$

Therefore

$$h_{sp} = \frac{D_0 - D_i - 2h_{sy}}{2}$$

$$h_{sp} = \frac{165.4 - 82.7 - (2 \times 12.84)}{2} = 28.51mm$$

f) Length of air gap (g)

The air gap length of this design is assumed to be 0.5mm for the

aligned position and 24.2mm for the unaligned position.

g) Rotor pole height (h_{rp})

The equation for the rotor pole height is mathematically expressed as;

$$h_{rp} = \frac{D_i - 2g - D_{sh} - 2h_{ry}}{2} = 14.59mm$$

2.3 Pulse Minimization

The control of the SRM is a combination of a rotor position sensing technique and an excitation circuit which supplied dc voltage to the winding on the stator. The rotor position sensing technique used is a commutation pulse generation scheme which was used to generate pulses for the phases A, B, C, in synchronization to the rotor angles of the SRM. Sensors like optical and hall sensors are only able to sense the position of the rotor at a fixed angle and not it's continuously changing angle, hence the use of this scheme which allows flexibility in the excitation angle. By modifying the turn on and turn off angles of the SRM, the aim to reduce the torque ripple could be achieved.

The torque and efficiency of the motor is dependent on the timing of the phase excitation. Windings with low phase angle produces maximum efficiency and vice versa. Controlling SRM also helps to control its speed and makes the stator phases to be well synchronized with the rotor poles. The winding excitation circuit is achieved using the circuit in Figure 3. The control topology was simulated in MATLAB Simulink environment.

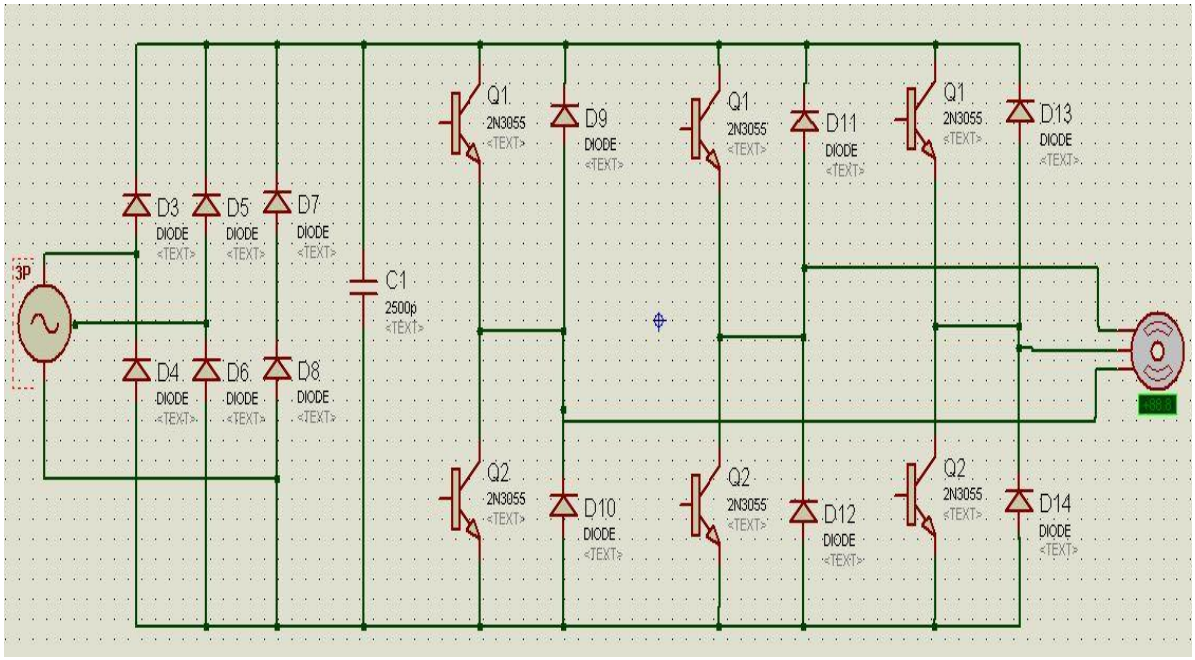

Figure 3: Winding Excitation Circuit Diagram of SRM

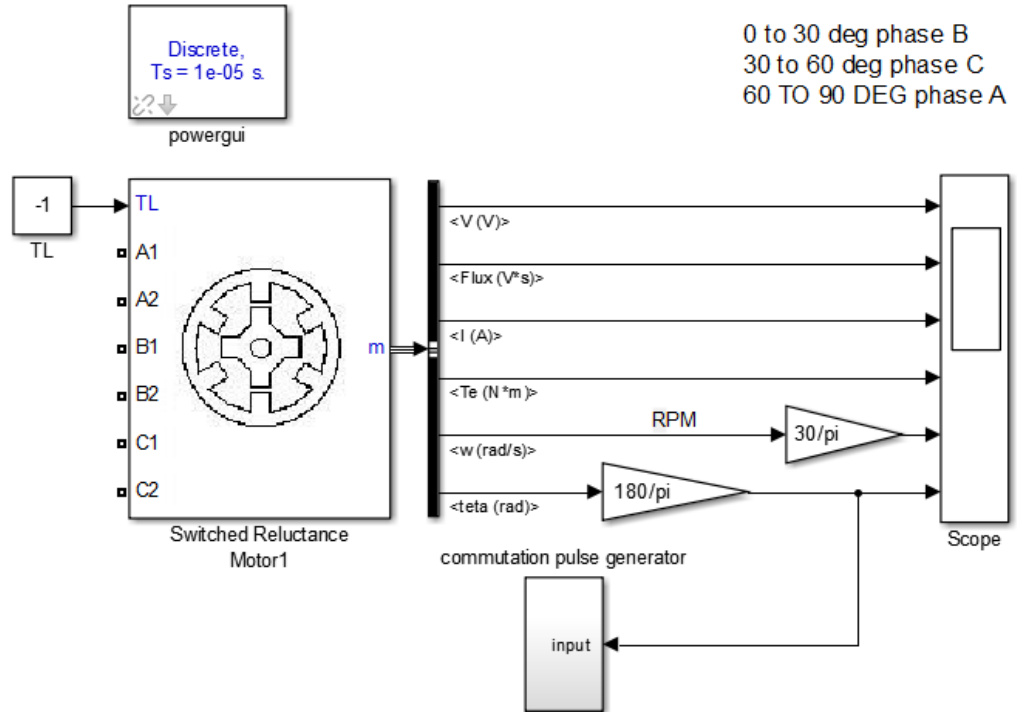

Figure 4. Simulink Block diagram of 6/4 Switched Reluctance Motor

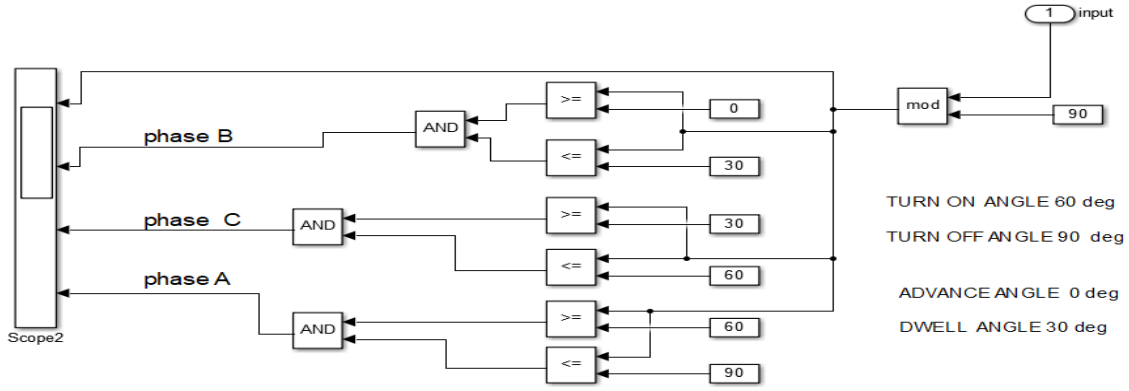

Figure 5: Simulink model for Commutation Generator with Zero degree Advance Angle.

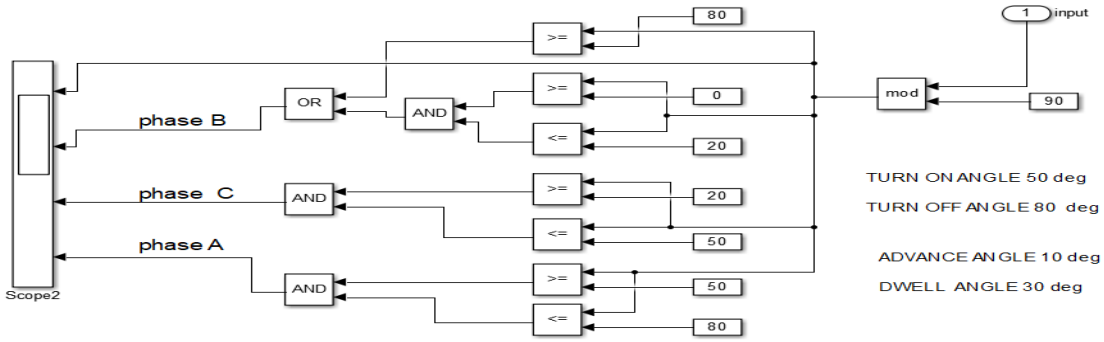

Figure 6. Simulink Model for Commutation Pulse Generator with Advance angle

Figures 4 to 6 show the Simulink model of pulse generation that has no advance angle application. The torque pulse minimization is achieved by advance angle of application of phase excitation.

3. Results and Discussion

3.1 Results

The results of the control topologies and analysis are shown from Figures 7 to 12. The excitation to the phases was supplied. Figure 7 shows the output of the control topology of SRM. Each of the phases is excited at different time based on the readings of the rotor sensor. Figure 8 shows the output waveform of the commutation pulse generator. The flux density distribution of the designed SRM was performed and the plot shown in Figure 9.

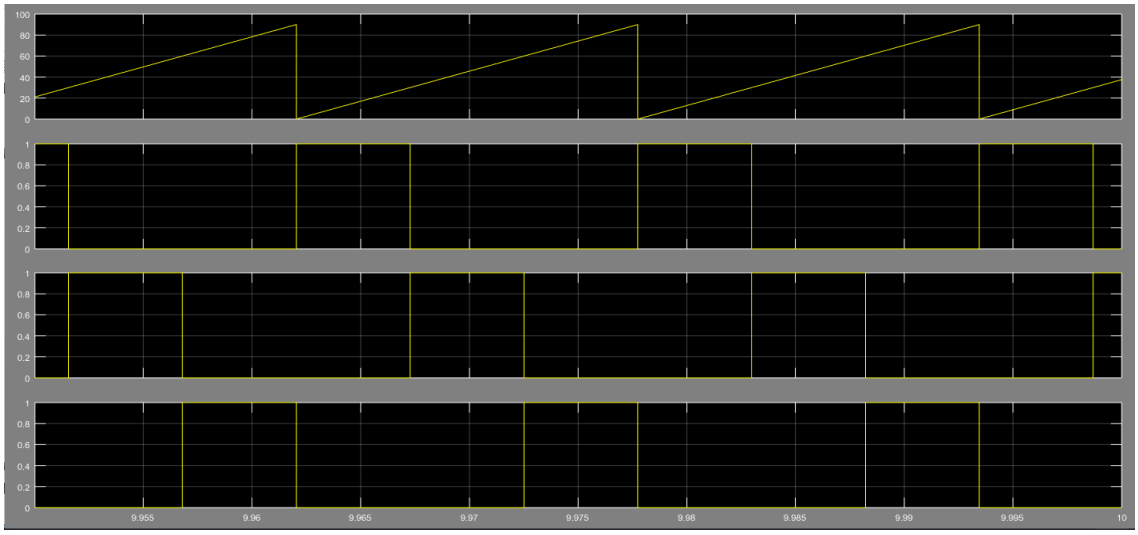

Figure 7: Switched Reluctance Motor Output using fixed Rotor Angle

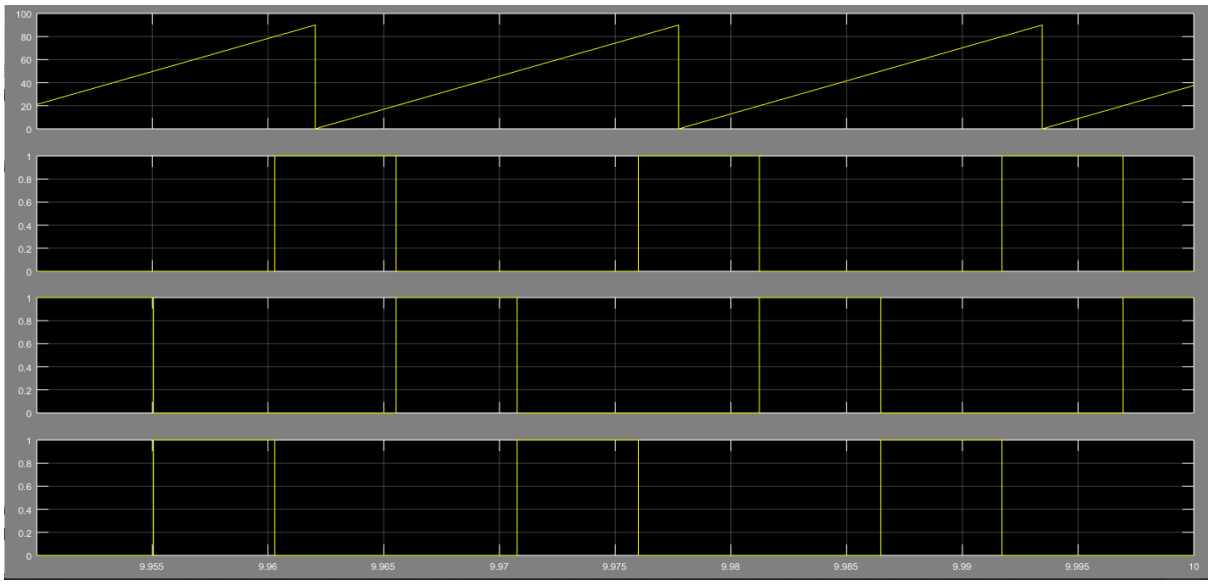

Figure 8:Output waveform of commutation pulse generator with flexible excitation angle

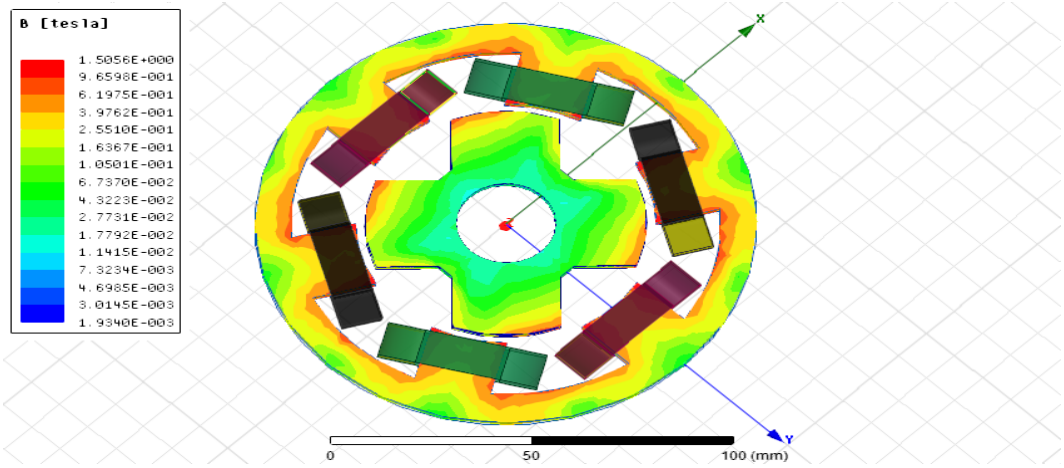

Figure 9: Flux distribution plot of Designed SRM

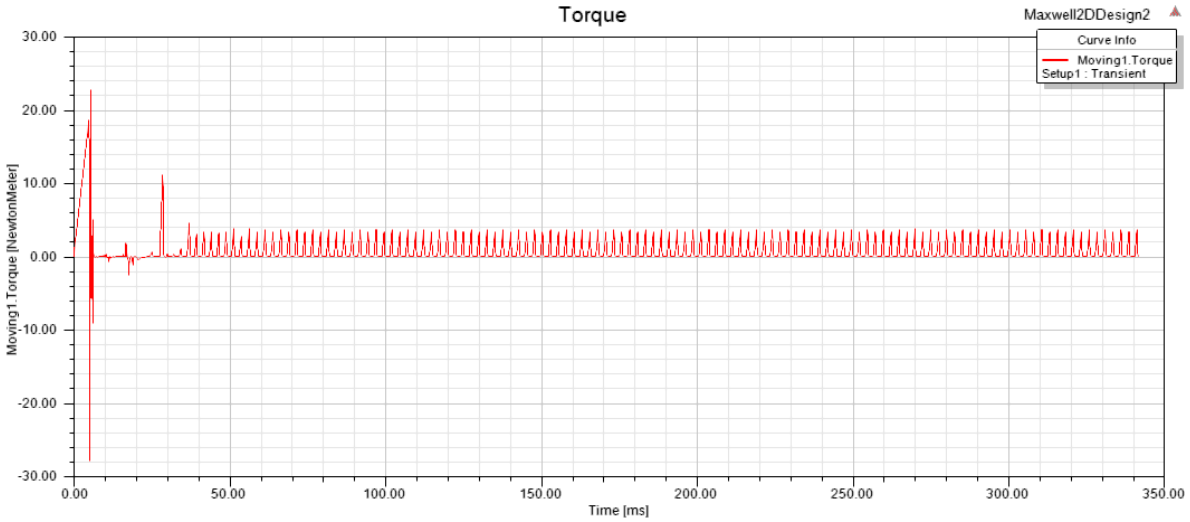

Figure 10: Torque plot of the designed SRM

Figure 11. Stator and Rotor development of SRM

Figure 12: Placement of Windings in the Stator

3.2 Discussion

The plot shown in Figures 7 and 8 presents the difference in using fixed excitation angle and advanced excitation angle of the phases. Figure 8 had its excitation of the next phase applied before the collapse of the previous phase excitation. This may help in reducing the torque pulsation. Figure 9 shows the flux density distribution and that the designed motor did not experience saturation in any part as the highest flux density recorded from the plot is 1.5 T, which is less than 1.8 T.

Conclusion

The three-phase switched reluctance motor was design and developed. The designed motor was analysed before the development so as to check the performance of the designed motor. The control topology was designed in such a way to reduce the acoustic noise and Torque pulsation. The results of the analysis conform to the standard performance of switched reluctance motor. The maximum Torque obtained was about 3.9 Nm as shown in Figure 10. The motor was developed according to the design. The ripple in the torque plots was reduced by applying the excitation to the phases in advance. The developed motor was shown in Figures 11 and 12. There are 6 poles on the stator which carries the windings and 4 poles on the rotor. There are no windings on the rotor.

References

Wang, G., Huang, L.., Zhao, X., Niu, H., & Dai, Z. (2006). Aliphatic and polycyclic aromatic hydrocarbons of atmospheric aerosols in five locations of Nanjing urban area, China. Atmospheric Research 81, 4583-4591.

Allirani S., Vidhya, H., Aishwarya, T., Kiruthika, T. and Kowsalya, V., (2018). "Design and Performance Analysis of Switched Reluctance Motor Using ANSYS Maxwell," *2018 2nd International Conference on Trends in Electronics and Informatics (ICOEI)*,1427-1432, doi: 10.1109/ICOEI.2018.8553912.

Bao J., Boynov, K., Paulides, J. and Lomonova,E., (2016). "Usage of the Inductive Energy Storage in the Field Winding for Driving the Variable Reluctance Motor," IEEE Transactions on Magnetics, 52(7): 1-4, doi: 10.1109/TMAG.2016.2527359.

Cao R., Su, E. and Lu, M., (2020). "Comparative Study of Permanent Magnet Assisted Linear Switched Reluctance Motor and Linear Flux Switching Permanent Magnet Motor for Railway Transportation," in IEEE Transactions on Applied Superconductivity, 30(4):1-5, doi: 10.1109/TASC.2020.2965874.

Chiang C.C., Hsieh,M., Li,F., Y.H. and Tsai,M.C., (2015). "Impact of Electrical Steel Punching Process on the Performance of Switched Reluctance Motors," IEEE Transactions on Magnetics, 51(11):1-4,doi: 10.1109/TMAG.2015.2449661.

Fan J. and Lee, Y., (2020). "Design Consideration to Achieve Wide-

Speed-Range Operation in a Switched Reluctance Motor," *Canadian Journal of Electrical and Computer Engineering*43(4):290-294, doi: 10.1109/CJECE.2020.2978265.

Farahani E. Farmahini, M., Jalali Kondelaji, A. and Mirsalim, M., (2020). "A New Exterior-Rotor Multiple Teeth Switched Reluctance Motor with Embedded Permanent Magnets for Torque Enhancement," in *IEEE Transactions on Magnetics*, 56(2):1-5, doi: 10.1109/TMAG.2019.2955884.

Jae-Hak Choi, J. S. Ahn and Ju Lee, (2005). "The characteristic analysis of switched reluctance motor considering DC-link Voltage ripple on hard and soft chopping modes," in IEEE Transactions on Magnetics, 41(10): 4096-4098, doi: 10.1109/TMAG.2005.854896.

Ji-Young L., Byoung-Kuk, L., Tao, S., Jung-Pyo, H. and Woo-Taik, L., (2006). "Dynamic Analysis of Toroidal Winding Switched Reluctance Motor Driven by 6-Switch Converter", IEEE Transactions on Magnetics, 42(4):1275-1278.

Kim J., Ha, K. and Krishnan, R., (2012). "Single-Controllable-Switch-Based Switched Reluctance Motor Drive for Low Cost, Variable-Speed Applications," in *IEEE Transactions on Power Electronics*, 27(1): 379-387,doi: 10.1109/TPEL.2011.2158239.

Krishnan R., (2001). *Switched Reluctance Motor Drives*. Boca Raton, FL: CRC Press, pp. 225 – 267

Krishnan R., Sung-Yeul P. and Keunsoo Ha., (2005) "Theory and operation of a four-quadrant switched reluctance motor drive with a single controllable switch-the lowest cost four-quadrant brushless motor drive," *in IEEE Transactions on Industry Applications*, 41(4): 1047-1055, doi: 10.1109/TIA.2005.851019.

Sanches E. S. and Santisteban J. A., (2015). "Mutual Inductances Effect on the Torque of an Axial Magnetic Flux Switched Reluctance Motor," *IEEE Latin America Transactions*, 13(7): 2239-2244, doi: 10.1109/TLA.2015.7273783.

Sato Y., (2007) "Development of a 2-Degree-of-Freedom Rotational/Linear Switched Reluctance Motor," IEEE Transactions on Magnetics,43(6):2564-2566, doi: 10.1109/TMAG.2007.892854.

Sheth N. K. and Rajagopal K. R., (2005). "Calculation of the flux-linkage characteristics of a switched reluctance motor by flux tube method," in IEEE Transactions on Magnetics, 41(10): 4069-4071,doi: 10.1109/TMAG.2005.854865.

Zou Y. K., Cheng W. E., Cheung,N. C. and Pan, J., (2014). "Deformation and Noise Mitigation for the Linear Switched Reluctance Motor With Skewed Teeth Structure," IEEE Transactions on Magnetics, 50(11):1-4, doi: 10.1109/TMAG.2014.2323420.